2011 International Nuclear Atlantic Conference - INAC 2011
Belo Horizonte,MG, Brazil, October 24-28, 2011
ASSOCIAÇÃO BRASILEIRA DE ENERGIA NUCLEAR - ABEN
***ISBN:* 978-85-99141-04-5**

OSL DATING RESULTS OF POST-BARREIRAS SEDIMENTS IN THE PARAÍBA BASIN, NORTHEASTERN BRAZIL

Diego R. G. Tudela[1], Juan C. R. Mittani[2], Sonia H. Tatumi[2], Dilce F. Rossetti[3] and Casimiro S. Munita[1]

[1] Instituto de Pesquisas Energéticas e Nucleares, IPEN - CNEN/SP
Av. Prof. Lineu Prestes, 2242 – Cidade Universitária –CEP 05508-000 São Paulo - SP - Brasil
drtudela@ipen.br

[2] Faculdade de Tecnologia de São Paulo (FATEC-SP / CEETEPS)
Laboratório de Datação e Luminescência de Cristais
Pça. Cel. Fernando Prestes, 30
01124-060 São Paulo, SP
tatumi@fatecsp.br

[3] Instituto Nacional de Pesquisas Espaciais (INPE)
Centro de Observação da Terra, Divisão de Sensoriamento Remoto - DSR
Rua dos Astronautas, 1758
12245-970 São José dos Campos, SP
rossetti@dsr.inpe.br

ABSTRACT

In the present study we show ages of 39 sediments samples of two sedimentary units (PB1 and PB2) collected from Paraíba Basin, northeastern Brazil, obtained by optically stimulated luminescence (OSL) making use of standardized growth curve (SGC) and applying single aliquot regenerative dose (SAR) protocol in 15 randomly selected samples to validate the equivalent Dose (D_e). Environmental radiation dosimetry of the area was performed to evaluate the natural concentrations of ^{238}U, ^{232}Th and ^{40}K and in this way annual dose rates of the locations were evaluated.

The results showed natural radioisotopes concentrations between 0.542-4.879 ppm for U, 1.314-26.098 ppm for Th and 0.141-1.12% for K and annual dose rates between 439-4172µGy/yr. The ages ranged from 1.8-178.3 kyr were obtained, and they are in agreements with the geological considerations.

1. INTRODUCTION

Optically Stimulated Luminescence (OSL) dating has been increasingly used by geologists for the establishment of sediment chronology. Luminescence dating has a limit of determination of 800 kyr (Figure 1) approximately, these limits are dependent on circumstances, for example, sample preservation, and also, the limits are liable to extend with continued technical development (Aitken, 1990). This technique has as advantage the covering of a large part of the Quaternary time frame (Figure 2). In particular, OSL dating has contributed to improve the chronological framework of important events that took place during this period, such as the glaciations episodes during the Pleistocene (Lomax *et al*, 2011;

Soares *et al*, 2010; Thamo-Bozso *et al*, 2010; Andreucci *et al*, 2010; Kaiser *et al*, 2010; Carneiro *et al*, 2002).

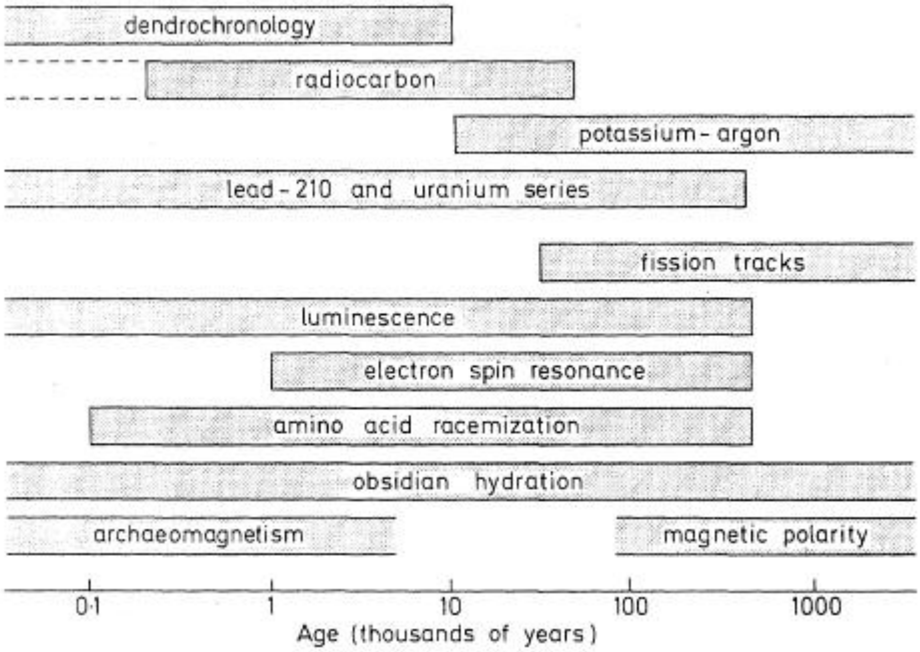

Figure 1. Methods and Age ranges (adapted from Aitken, 1990).

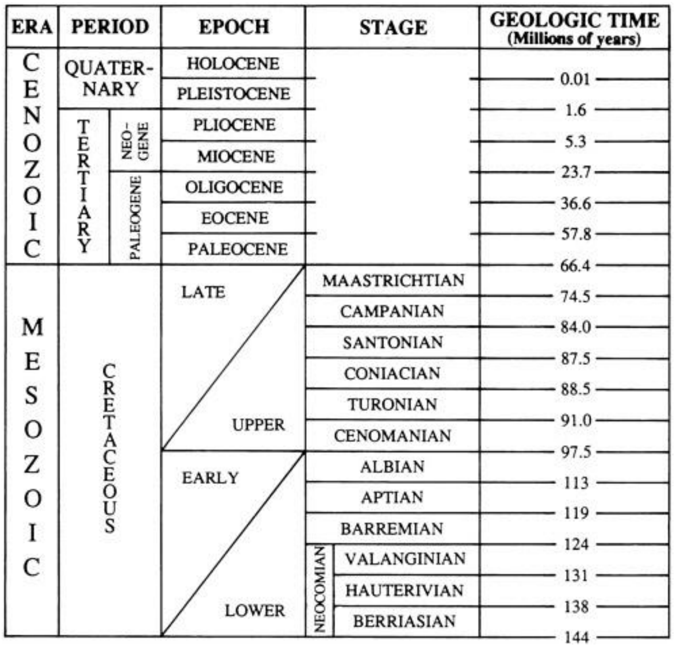

Figure 2. Geological time scale from Cretaceous to Quaternary periods (Palmer, 1983).

The OSL dating technique determines the time elapsed since sediment grains were last exposed to sun light. This exposure time resets the luminescence signal of some grains, such as quartz and feldspar, a process known as bleaching. While buried quartz grains are protected from light, they are exposed to ionizing radiation from radionuclides naturally present in the soil. The radionuclides increase the luminescence signal of these minerals, with the intensity of the signal dependent of ionizing flux and directly proportional to the time interval when they remained buried. The theory of crystal luminescence and their application for dating was described in detail by Aitken (1998).

In order to determine the sediment age, i.e., the time elapsed from the last exposure of quartz grains to light, it is necessary to know the amount of dose acquired by them along the time from naturally occurring radioactivity until present. This is commonly referred as equivalent dose (D_e), given in Gy (J/Kg). The dose absorbed by the grains during a period of one year, is called annual dose rate (AD), given in Gy/year, and it is calculated by measuring the concentrations of radionuclides naturally present in the soil. The sediment age (A) is obtained by dividing the equivalent dose by the annual dose rate.

$$A = \frac{D_e}{AD} \frac{(Gy)}{\left(Gy / Year \right)} \tag{1}$$

To determine D_e it is necessary to apply a known laboratory dose, calculate the OSL intensity or area under the OSL curve, and then compare the results to the natural OSL response. This will provide an accurate value of D_e. However, estimations of D_e for quartz grains required many aliquots (i.e., 50~100, about 10 mg each) (Murray and Olley, 2002) to find only one age.

Murray and Wintle (2000) and Wintle (2008) improved the single aliquot regenerative dose (SAR) protocol previously proposed by other authors (e.g., Galbraith *et al*, 1999; Hilgers *et al*, 2001; Murray and Roberts, 1998). In this improved protocol is possible to monitor and correct changes in sensitivity of OSL natural or regenerative measurements using the OSL response to a test dose (~10 to 20% of D_e) (Murray and Wintle, 2000). This protocol has the advantage that it requires a little amount of sample, which results in more accurate values of D_e and, subsequently more precise age.

In this paper the OSL ages were obtained by the standardized growth curve methods (Roberts and Duller, 2004), as well as Single Aliquot Regenerative Dose (SAR) to validate D_e in 15 samples.

The studied samples derived from the Quaternary Post-Barreiras Sediments of the Paraiba Basin were selected for this test due to its geological importance to study the interplay among tectonic, sedimentations and landforms, associated with the evolution of the South American passive margin after continental breakup (Rossetti *et al*, 2011)

2. EXPERIMENTAL METHODS

This study was based on the Optically Stimulated Luminescence (OSL) dating of thirty nine sediment samples of the Post-Barreiras Sediments from the Paraíba Basin, northeastern, Brazil (Figure 3). All samples were undergone to cleansing applying chemical treatments with H_2O_2, HF and HCl. Following this step, the samples were sieved to obtain grain sizes between 125 and 180 µm. Samples within this grain size range were treated with Sodium Politungstate (SPT) calibrated to quartz density in order to separate quartz grains.

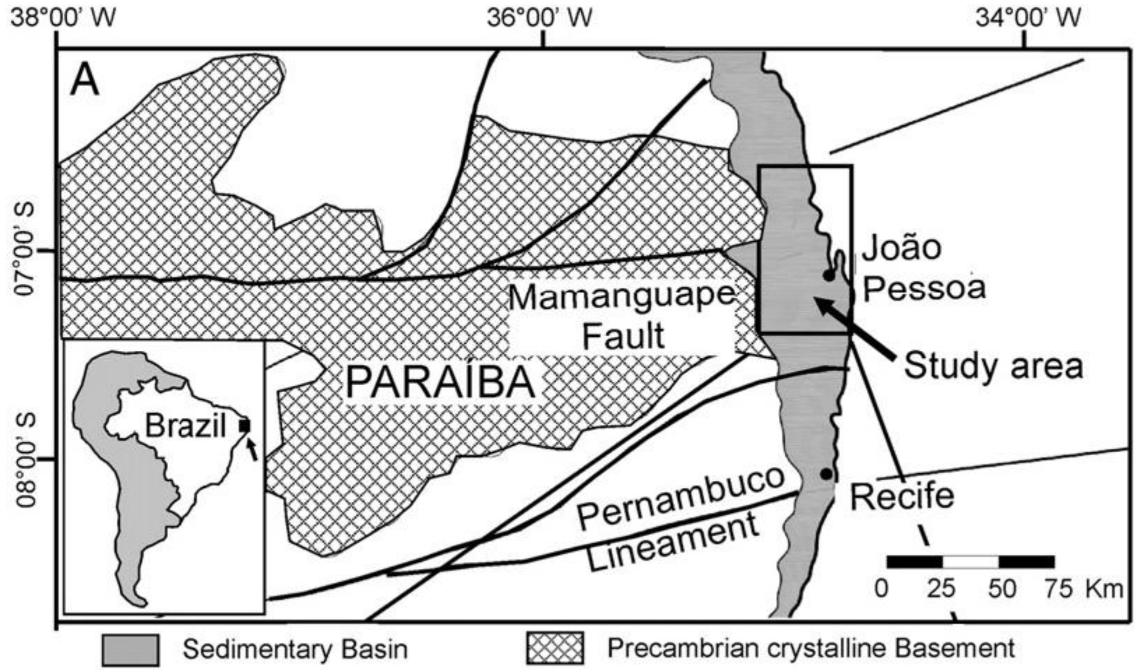

Figure 3. Map of the study area in the central part of the Paraíba Basin, northeastern Brazil (Rossetti *et al*, 2011).

A total of 15 samples were dated employing the SAR protocol. It is necessary to ensure that the samples do not lose weight during the process of successive irradiation/measurements cycles required in the SAR protocol. To avoid mass loss, we designed and built a pellet maker (Tatumi *et al*, 2008). The samples (about 6-7 mg of quartz for each aliquot) were deposited on polytetrafluorethylene surfaces (100 mg of PTFE) and then pressed (Figure 4A and 4B). From each sample 10 aliquots were obtained, which resulted in 10 ages per sample.

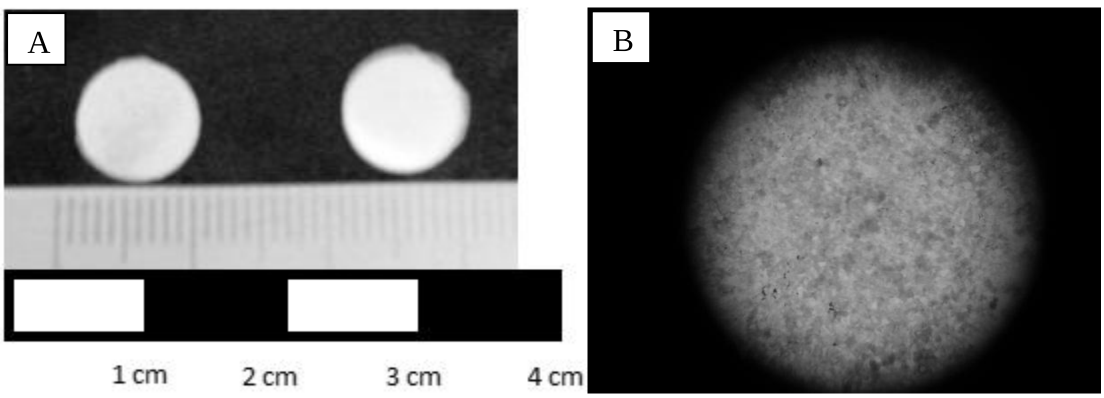

Figure 4. PTFE with quartz deposited on surface. A) Zoom 1x. B) Zoom 20x.

The γ-irradiation was performed using a ^{60}Co source at the Instituto de Pesquisas Energéticas e Nucleares, (IPEN - CNEN/SP). The isotopic content of natural radionuclides were determined with gamma spectroscopy, using a portable Inspector Spectroscopy workstation, with NaI(Tl) detector model 802 of Canberra and lead shield model 727. The data were calibrated with JG-1a, JA-3, JB-2, and JB-3 Japanese's soil standard samples. Peak energies used 238, 352, 1120, 1460, 1760 and 2620 KeV. The annual dose rates were calculated using the activity concentration from ^{232}Th, ^{238}U and ^{40}K, determined by gamma spectroscopy and Bell's equation. OSL dating was carried out with an incorporated DayBreak Nuclear and Medical Systems, Model 1100–series automated TL/OSL system.

OSL dating of quartz grains was performed using a blue light diode (~470 nm) and the detection through ~5 mm Hoya U-340 optic filter in front of the PMT. The OSL ages were obtained by standardized growth curve (SGC) method. Single aliquot regenerative dose (SAR) protocol was also used but only in 15 random samples to validate the equivalent dose (D_e). The natural luminescence signal (L_n) and the laboratory test dose (T_n) were measure for the SGC. The ratio of both signals (L_n/T_n) was multiplied by the size of the test dose applied $(L_n/T_n)*T_d$, in order to obtain the standardized OSL signal. Samples were preheated at 250 °C for 10 s prior measurements, and at 200 °C for 10 s after the test dose. The same thermal treatments were used during SAR protocol.

To build SGC, eight different doses between 10 and 600 Gy were used (Figure 5), with five aliquots measured for each dose. To obtain the convenient De, a regression curve using the equation (2) was fitted through the data.

$$(OSL) = I_{\max}\left(1 - e^{-D/D_0}\right) + K.D \qquad (2)$$

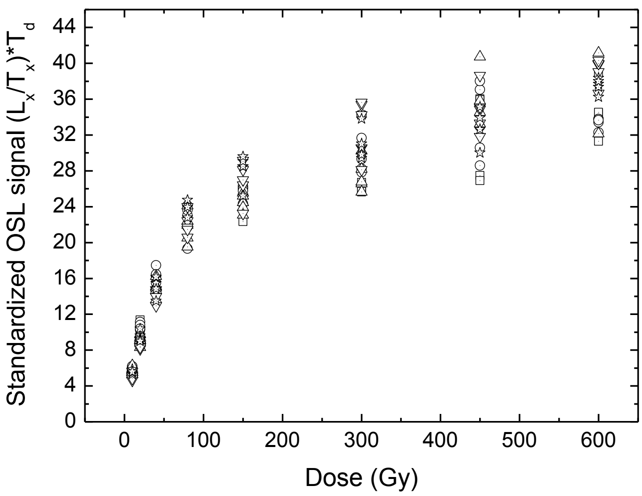

Figure 5. Standardized growth curve (SGC) used to obtain OSL ages.

3. RESULTS AND DISCUSSION

Table 1 shows the OSL ages obtained and values of U, Th and K. The U contents in the samples are show in Figure 6, with a mean value of 2.04 (±1.2) ppm, fitted with Gauss equation, and a peak value of 1.565 (±0.291) ppm. The mean value of Th contents was 8.98 (±7.08) ppm, however frequency distribution could not be fitted with Gauss equation (Figure 7). The rate of U/Th is shown in Figure 8. The majority of the samples have this rate lower than 0.3. The ^{40}K content in the samples was very low, the majority being 0.2% with a mean value of 0.34 (±0.27) % (Figure 9).

Table 1. OSL ages obtained of the post-Barreiras Sediments

Unit	Sample	U (ppm)	Th (ppm)	K (%)	D_e (Gy)	AD (µGy/yr)	Age (Kyr)
PB1	PB1-7	2.643	11.748	0.298	31.4	2068±84	15.2±1.4
	PB1-8	2.237	9.200	0.151	40.2	1622±50	24.8±2.0
	PB2-8	1.510	7.228	0.151	71.0	1416±80	50.2±5.4
	PB2-9	2.094	9.058	0.505	44.5	2090±183	21.3±2.9
	PB2-10	3.207	15.313	b.d.l	48.0	2590±217	18.5±2.5
	PB3-8	2.455	10.917	0.462	60.0	2126±102	28.0±4.0
	PB3-13	1.423	6.142	0.550	49.0	1591±142	30.8±6.9
	PB3-14	1.098	3.878	0.272	51.0	1053±74	48.4±5.1
	PB4-3	0.542	1.168	b.d.l	19.2	511±6	37.6±2.3
	PB4-4	1.080	1.278	b.d.l	20.0	439±35	45.6±5.9
	PB5-1	0.611	1.242	0.426	31.5	1003±219	31.4±8.4
	PB6-1	0.720	0.753	b.d.l	23.4	492±20	47.5±4.3
	PB6-2	0.472	0.724	0.093	29.4	521±76	56.4±11.1
	PB7-1	2.720	12.862	0.533	184.0	2413±118	76.0±9.1
	PB7-2	2.493	12.143	0.589	85.0	2358±123	36.0±2.8
	PB7-3	0.884	2.081	0.524	28.0	1122±116	25.0±2.7
	PB8-1	2.046	7.508	0.549	125.0	1853±165	67.5±9.2
	PB8-2	1.226	3.691	0.188	18.0	968±57	19.0±1.9
	PB8-10	1.937	6.437	0.282	70.0	1471±134	48.0±5.1
	PB8-11	2.444	12.738	0.396	78.0	2192±125	35.6±3.4
	PB9-4	3.051	14.502	0.538	39.6	2613±185	15.2±1.8
	PB9-5	0.785	1,314	b.d.l	26.9	551±50	48.8±6.9
	PB10-3	2.021	8.655	0.284	51.9	1662±151	31.2±4.4
	PB11-1	0.683	1.353	b.d.l	11.2	521±42	21.5±2.8
	PB12-2	2.124	9.950	0.211	39.2	1769±159	22.3±3.1
	PB12-3	1.628	7.842	0.467	27.0	1686±112	16.0±1.9
	PB13-2	3.935	18.265	0.899	53.0	3506±240	15.1±1.8
	PB13-5	3.637	19.442	0.460	131.3	3068±159	42.8±4.4
	PB13-7	4.477	23.062	0.607	213.5	3703±189	57.6±5.8
	PB14-1	0.715	1.410	b.d.l	11.2	521±42	21.5±2.8
	PB15-4	4.879	26.098	0.738	116.6	4172±340	27.9±3.7
	PB15-5	4.031	18.952	1.120	285.0	3809±283	74.8±9.3
	PB16-3	2.799	15.553	0.638	489.0	2743±276	178.3±26.8
PB2	PB1-5	1.298	5.446	0.141	9.6	1088±53	8.8±0.9
	PB1-6	1.674	5.903	0.578	18.9	1667±165	11.3±1.7
	PB3-10	1.547	5.129	0.245	2.5	1235±58	2.0±0.2
	PB3-11	1.419	4.496	0.219	2.0	1128±54	1.8±0.2
	PB8-3	0.754	2.194	0.215	4.6	780±42	6.0±0.6
	PB9-3	4.366	24.443	b.d.l	15,1	3299±168	4.6±0.5

b.d.l = below detection limit.

In general, deposits characterized by mineralogical composition consisting mainly of quartz and plagioclase have low concentration of K, U and Th, while deposits consisting of mica, feldspar, monazite and apatite, contain higher levels of these elements. Hence, with the increase of silica content, there is a decrease in K, U and Th contents.

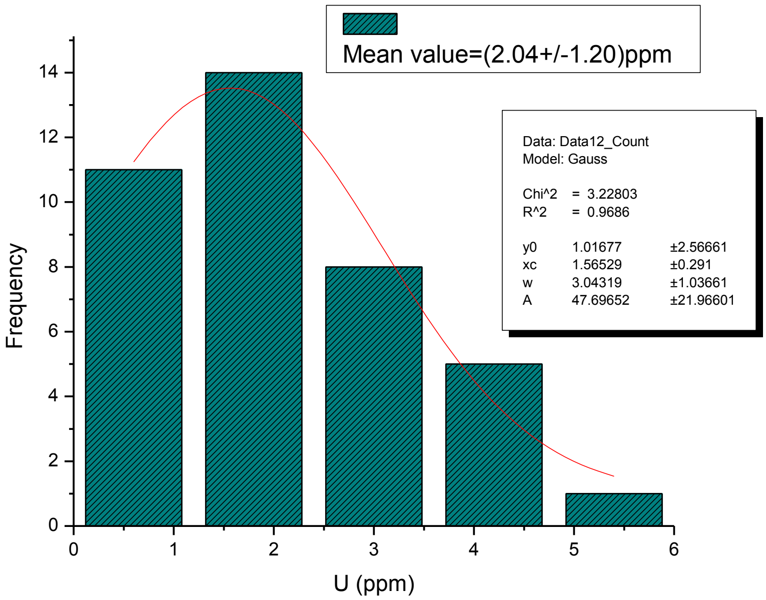

Figure 6. Frequency of U contents fitted with Gauss Equation.

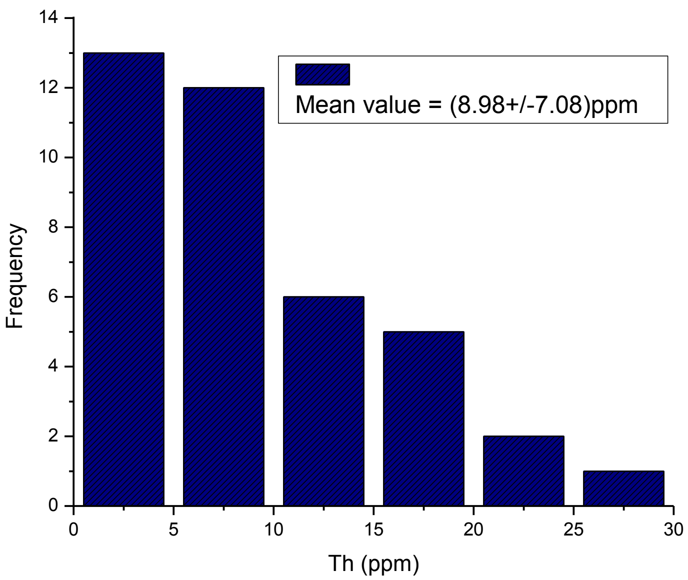

Figure 7. Frequency of Th contents.

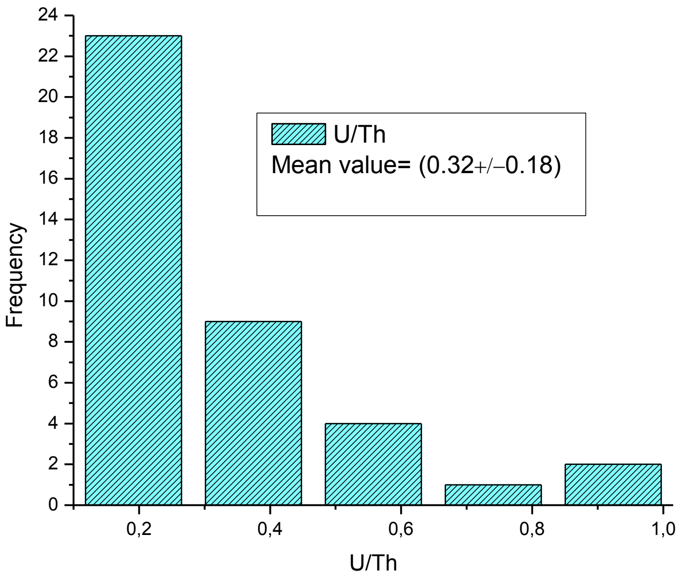

Figure 8. U/Th rate.

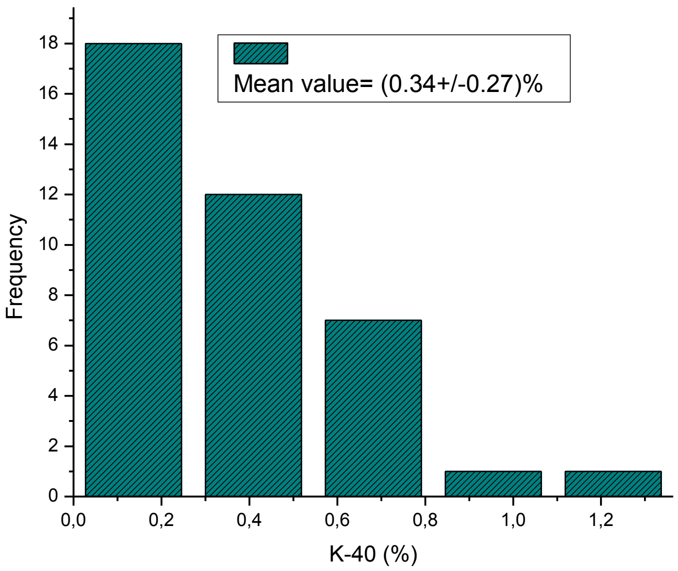

Figure 9. ^{40}K content.

The accuracy and precision of ages obtained by luminescence dating depend of the bleaching rate of fast component of OSL from quartz grains exposed to sun light and a careful cleaning of the samples. However, the most important influence factor is the type of environmental setting where the grains were transported and deposited. Bleaching rates vary according to depositional process, thus obtained ages from quartz grains deposited in some environments might be troublesome.

Aeolian depositions have the most potential to provide complete bleaching, while subaqueous environments might vary depending on flow behavior. About this issue Murray and Olley (2002) presents a series of tests about depositional process.

In the instance of samples analyzed in this study we assume that bleaching during deposition process was sufficient to provide consistent OSL ages, as observed by their increase with depth along stratigraphic profiles (the only exception being sample PB16-3, with age of 178.3 Ka, which resulted in an age much older than obtained in any of the other samples, as seen in the Figure 10 below, which are shown the OSL ages histogram distributed in columns and frequency counts).

These results are in agreement with the proposed environmental setting proposed for these deposits, which include mostly aeolian and alluvial deposition. It has been proposed, however, that the Post-Barreiras Sediments have also a shallow marine contribution (Rossetti *et al*, 2011). If this interpretation is correct, subaqueous deposition in shallow marine environments did not affect grain bleaching.

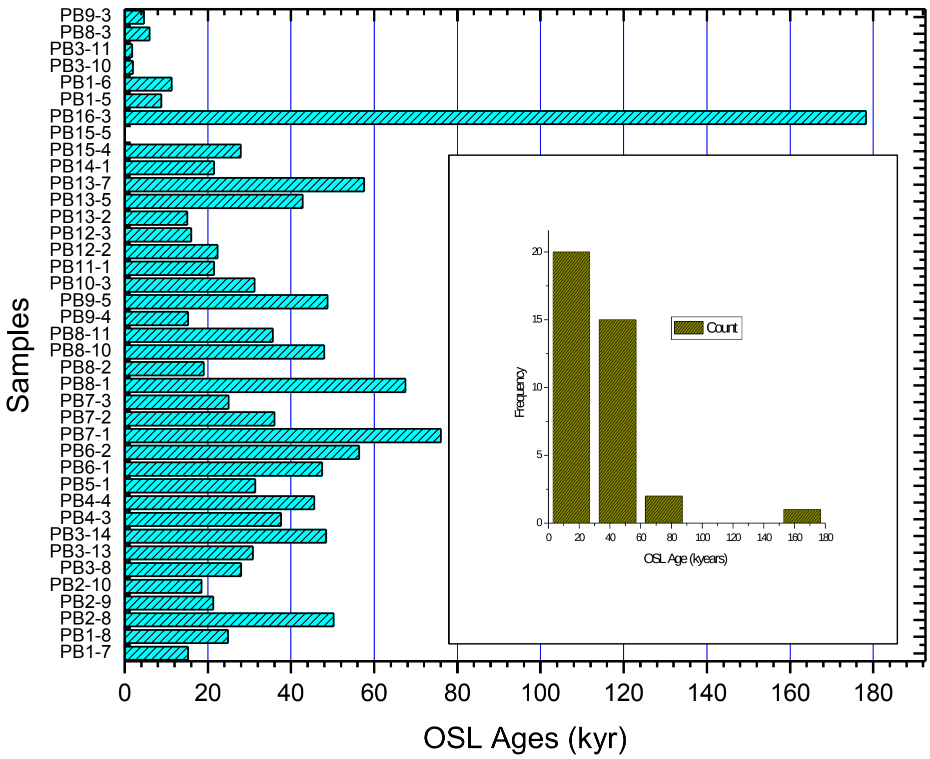

Figure 10. OSL ages histogram.

4. CONCLUSIONS

The OSL ages obtained for the studies deposits showed results consistent along the lithostratigraphic profiles and also when profiles from different areas were compared. These data are also in agreement with the geological context proposed for the studied deposits, which are inserted within the Post-Barreiras Sediments, interpreted to have deposited within the latest Quaternary time frame.

Additionally, the results helped to distinguish two subunits within these deposits, the PB1 and PB2, formed during the Late Pleistocene and mostly Holocene, respectively.

5. REFERENCES

1. M. J. Aitken, *Science-based Dating in Archaeology*, Longman, London, UK (1990).
2. J. Lomax, A. Hilgers, U. Rodtke, "Palaeoenvironmental change recorded in the paleodunefields of the western Murray Basin, south Australia – New data from single grain OSL-dating," *Quaternary Science Reviews*, **30**, pp.723-736 (2011).
3. E. A. A. Soares, S. H. Tatumi, C. Riccomini, "OSL age determination of Pleistocene fluvial deposits in Central Amazonia," *Anais da Academia Brasileira de Ciências*, **82 (3)**, pp.691-699 (2010).
4. E. Thamo-Bozso, M. Arpad, M. Balazs, A. Nagy, "OSL ages and origin of Late Quaternary sediments in the North Transdanubian Hills (Hungary): timing of neotectonic activity," *Quaternary International*, **222 (1-2)**, pp.209-220 (2010).
5. S. Andreucci, L. B. Clemmensen, A. S. Murray, V. Pascucci, "Middle to Late Plesitocene coastal deposits of Alghero, northwest Sardinia (Italy): Chronology and evolution," *Quaternary International*, **222 (1-2)**, pp.3-16 (2010).
6. K. Keiser, Z. P. Lai, B. Schneider, F. W. Junge, "Late Pleistocene genesis of the middle Yarlung Zhangbo Valley, southern Tibet (China), as deduced by sedimentological and luminescence data," *Quaternary Geochronology*, **5 (2-3)**, pp.200-204 (2010).
7. A. Carneiro, D. Schwartz, S. H. Tatumi, T. Rosique, "Amazonian paleodune provide evidence for drier climate phases during Late Pleistocene-Holocene," *Quaternary Research*, **58 (2)**, pp.205-209 (2002).
8. A. R. Palmer, "The Decade of North American Geology – 1983 Geologic Time Scale," *Geology*, **11**, pp.503-504 (1983).
9. M. J. Aitken, *An Introduction to Optical Dating*, Oxford University Press, New York. USA (1998).
10. A. S. Murray, J. M. Olley, "Precision and Accuracy in the Optically Stimulated Luminescence Dating of Sedimentary Quartz: A Status Review," *Geochronometria*, **21**, pp.1-16 (2002).
11. A. S. Murray, A. G. Wintle, "Luminescence dating of quartz using an improved single-aliquot regenerative-dose protocol," *Radiation Measurements*, **32**, pp.57-73 (2000).
12. A. G. Wintle, "Fifty years of Luminescence Dating", *Archaeometry*, **50**, pp.276-312 (2008).
13. R. Galbraith, R. G. Roberts, G. Laslett, H. Yoshida, J. Olley, "Optical dating of single and multiple grains of quartz from jinmium rock shelter, Northern Autralia. Part I: Experimental Design and Statistical Models," *Archaeometry*, **41**, pp.339-364 (1999).
14. A. Hilgers, A. S. Murray, N. Schlaak, U. Radtke, "Comparison of quartz OSL protocols using Lateglacial and Holocene dune sands from Brandenburg, Germany," *Quaternary Geochronology*, **20**, pp.731-736 (2001).
15. A. S. Murray, R. G. Roberts, "Measurement of equivalent dose in quartz using a regenerative-dose single-aliquot protocol," *Radiation Measurements*, **29**, pp.503-515 (1998).

16. H. M. Roberts, G. A. T. Duller, “Standardized growth curves for optical dating of sediment using multiple grain aliquots,” *Radiation Measurements*, **38**, pp.241-252 (2004).
17. D. F. Rossetti, F. H. R. Bezerra, A. M. Góes, M. M. Valeriano, C. O. Andrades-Filho, J. C. R. Mittani, S. H. Tatumi, B. B. B. Neves, “Late Quaternary sedimentation in the Paraíba Basin, Northeastern Brazil: Landform, sea level and tectonics in Eastern South America passive margin,” *Palaeogeography, Palaeoclimatology, Palaeoecology*, **300**, pp.191-204 (2011).
18. S. H. Tatumi, L. P. Silva, Pires, E.L., Rossetti, D.F., Góes, A.M., Munita, C.S., “Datação de Sedimentos Pós-Barreiras no Norte do Brasil: implicações paleogeográficas”, *Revista Brasileira de Geociências*, **38 (3)**, pp514-524 (2008).